Please cite this article in press as: Davis et al., The Somatic Genomic Landscape of Chromophobe Renal Cell Carcinoma, Cancer Cell (2014), http://dx.doi.org/10.1016/j.ccr.2014.07.014

Cancer Cell
Article

The Somatic Genomic Landscape of Chromophobe Renal Cell Carcinoma

Caleb F. Davis,[1,34] Christopher J. Ricketts,[2,34] Min Wang,[1,34] Lixing Yang,[3,34] Andrew D. Cherniack,[4] Hui Shen,[5] Christian Buhay,[1] Hyojin Kang,[32] Sang Cheol Kim,[6] Catherine C. Fahey,[7] Kathryn E. Hacker,[7] Gyan Bhanot,[8,9] Dmitry A. Gordenin,[10] Andy Chu,[11] Preethi H. Gunaratne,[1,12] Michael Biehl,[13] Sahil Seth,[14] Benny A. Kaipparettu,[15,16] Christopher A. Bristow,[14] Lawrence A. Donehower,[1] Eric M. Wallen,[17] Angela B. Smith,[17] Satish K. Tickoo,[18] Pheroze Tamboli,[19] Victor Reuter,[18] Laura S. Schmidt,[2,20] James J. Hsieh,[21,22] Toni K. Choueiri,[23,24] A. Ari Hakimi,[25] The Cancer Genome Atlas Research Network, Lynda Chin,[4,14] Matthew Meyerson,[4,23] Raju Kucherlapati,[26,27] Woong-Yang Park,[6,28] A. Gordon Robertson,[11] Peter W. Laird,[5] Elizabeth P. Henske,[4,23,24] David J. Kwiatkowski,[4,23,24] Peter J. Park,[3,26] Margaret Morgan,[1] Brian Shuch,[33] Donna Muzny,[1] David A. Wheeler,[1] W. Marston Linehan,[2] Richard A. Gibbs,[1] W. Kimryn Rathmell,[17,29,30,35,*] and Chad J. Creighton[1,15,31,35,*]

[1]Human Genome Sequencing Center, Baylor College of Medicine, Houston, TX 77030, USA
[2]Urologic Oncology Branch, Center for Cancer Research, National Cancer Institute, CRC Room 1W-5940, Bethesda, MD 20892, USA
[3]Center for Biomedical Informatics, Harvard Medical School, Boston, MA 02115, USA
[4]The Eli and Edythe L. Broad Institute of Massachusetts Institute of Technology and Harvard University, Cambridge, MA 02142, USA
[5]USC Epigenome Center, University of Southern California, Los Angeles, CA 90033, USA
[6]Samsung Genome Institute, Samsung Medical Center, Seoul, Korea
[7]Curriculum in Genetics and Molecular Biology, Lineberger Comprehensive Cancer Center, University of North Carolina, Chapel Hill, NC 27599, USA
[8]Department of Molecular Biology and Biochemistry, Rutgers University, Busch Campus, Piscataway, NJ 08854, USA
[9]Cancer Institute of New Jersey, 195 Little Albany Street, New Brunswick, NJ 08903, USA
[10]National Institute of Environmental Health Sciences, 111 T.W. Alexander Drive, Research Triangle Park, NC 27709, USA
[11]Canada's Michael Smith Genome Sciences Centre, BC Cancer Agency, Vancouver BC V5Z 4S6, Canada
[12]Department of Biology & Biochemistry, University of Houston, 4800 Calhoun Road, Houston, TX 77204, USA
[13]Johann Bernoulli Institute for Mathematics and Computer Science, Intelligent Systems Group, University of Groningen, P.O. Box 407, 9700 AK Groningen, the Netherlands
[14]Department of Genomic Medicine, Institute for Applied Cancer Science, The University of Texas MD Anderson Cancer Center, Houston, TX 77030, USA
[15]Dan L. Duncan Cancer Center, Baylor College of Medicine, Houston, TX 77030, USA
[16]Department of Molecular and Human Genetics, Baylor College of Medicine, Houston, TX 77030, USA
[17]Department of Urology, University of North Carolina, Chapel Hill, NC 27599, USA
[18]Department of Pathology, Memorial Sloan-Kettering Cancer, 1275 York Avenue, New York, NY 10065, USA
[19]Department of Pathology, The University of Texas MD Anderson Cancer Center, 1515 Holcombe Boulevard, Houston, TX 77030, USA
[20]Leidos Biomedical Research, Basic Science Program, Frederick National Laboratory for Cancer Research, Frederick, MD 21702, USA
[21]Department of Medicine, Weill-Cornell Medical College, New York, NY 10021, USA
[22]Human Oncology and Pathogenesis Program, Memorial Sloan-Kettering Cancer Center, New York, NY 10065, USA
[23]Department of Medical Oncology, Dana-Farber Cancer Institute, 450 Brookline Avenue, Boston, MA 02215, USA
[24]Department of Medicine, Harvard Medical School, Boston, MA 02215, USA
[25]Department of Surgery, Urology Service, Memorial Sloan-Kettering Cancer Center, New York, NY 10065, USA
[26]Department of Genetics, Harvard Medical School, Boston, MA 02115, USA
[27]Division of Genetics, Brigham and Women's Hospital, Boston, MA 02115, USA
[28]Sungkyunkwan University School of Medicine, Seoul, Korea
[29]Department of Genetics, University of North Carolina at Chapel Hill, Chapel Hill, NC 27599, USA
[30]Division of Hematology and Oncology, Department of Medicine, University of North Carolina, Chapel Hill, NC 27599, USA
[31]Department of Medicine, Baylor College of Medicine, Houston, TX 77030, USA
[32]National Institute of Supercomputing and Networking, Korea Institute of Science and Technology Information, Daejeon, Korea
[33]Department of Urology, Yale School of Medicine, New Haven, CT 06520, USA
[34]Co-first author
[35]Co-senior author
*Correspondence: rathmell@med.unc.edu (W.K.R.), creighto@bcm.edu (C.J.C.)
http://dx.doi.org/10.1016/j.ccr.2014.07.014

SUMMARY

We describe the landscape of somatic genomic alterations of 66 chromophobe renal cell carcinomas (ChRCCs) on the basis of multidimensional and comprehensive characterization, including mtDNA and whole-genome sequencing. The result is consistent that ChRCC originates from the distal nephron compared with other kidney cancers with more proximal origins. Combined mtDNA and gene expression analysis implicates changes in mitochondrial function as a component of the disease biology, while suggesting

alternative roles for mtDNA mutations in cancers relying on oxidative phosphorylation. Genomic rearrangements lead to recurrent structural breakpoints within *TERT* promoter region, which correlates with highly elevated *TERT* expression and manifestation of kataegis, representing a mechanism of *TERT* upregulation in cancer distinct from previously observed amplifications and point mutations.

INTRODUCTION

Rare tumor types offer a unique opportunity to investigate and discover mechanisms of tumorigenesis. Chromophobe renal cell carcinoma (ChRCC) is a subtype of renal cell carcinoma (RCC), representing ~5% of this heterogeneous group of cancers arising from the nephron (Störkel et al., 1997), with 3,000 new cases annually in the United States (Jemal et al., 2013). Although ChRCC typically exhibits an indolent pattern of local growth, with greater than 90% 10-year cancer-specific survival (Amin et al., 2002; Przybycin et al., 2011), aggressive features and metastasis can occur. ChRCC is associated with a distinct aneuploidy pattern (Speicher et al., 1994); however, genome-wide evaluation of its somatic mutation spectrum has not been reported. ChRCC is associated with germline mutation of *FLCN* in the autosomal-dominant cancer predisposition Birt-Hogg-Dubé (BHD) syndrome, in which 34% of BHD-associated kidney tumors are ChRCC (Nickerson et al., 2002; Pavlovich et al., 2002; Schmidt et al., 2001), and with germline mutation of *PTEN* in Cowden syndrome (Shuch et al., 2013). Previous studies have suggested a nonglycolytic metabolic profile for ChRCC, using ^{18}F-fluorodeoxyglucose positron emission tomography/computed tomography (Ho et al., 2012), and have shown that the genomic profile comprises unique whole-chromosome losses rather than focal events (Speicher et al., 1994).

Genomic profiling of rare cancers, such as ChRCC, can provide a more complete picture of the disease. Although very large sample numbers (>5,000) may be needed for some disease types in order to detect rare mutational events (Lawrence et al., 2014), in many cases, there remain undiscovered frequent mutations that drive disease. When data integration across multiple platforms is applied, patterns observed in one data type may be reflected in the other data types, building a more conclusive set of findings with regard to revealing driver events. For example, early DNA microarray studies of breast cancer, for example, globally assaying a single data type for 65 tumors (Perou et al., 2000) and incorporating clinical data, have had an enduring impact on our understanding of breast and other cancers, while *PBRM1* mutations were discovered in clear cell kidney cancers from an initial analysis of just 25 tumors (Varela et al., 2011). Understudied cancers, such as ChRCC, may hold this potential for discovery as well.

RESULTS

Copy-Number and Whole-Exome Analysis

The Cancer Genome Atlas (TCGA) collected a total of 66 primary ChRCC specimens (Table S1 available online) with matching normal tissue/blood, in order to better characterize the molecular basis of this cancer using multiple data platforms (Table 1; Table S1). Our comprehensive analysis of ChRCC involved a systematic examination by data type, including copy number and whole-exome sequencing (WES). By SNP array analysis, loss of one copy of the entire chromosome, for most or all of chromosomes 1, 2, 6, 10, 13, and 17, was seen in the majority of cases (86%; Figure 1A). Losses of chromosomes 3, 5, 8, 9, 11, 18, and 21 were also noted at significant frequencies (12%–58%). There were no focal copy-number events by GISTIC analysis (Mermel et al., 2011), suggestive of a simpler chromosomal landscape for ChRCC in comparison with that of other cancers, including the more common clear cell type RCC (ccRCC). We subdivided our ChRCC cases according to previously defined histologic categories of "classic" (n = 47), which demonstrate the classical pale cytoplasmic features for which the disease was named, and "eosinophilic" (n = 19), based on abundant, eosinophilic cytoplasm and densely packed mitochondria, by expert consensus pathology review (Brunelli et al., 2005). Although all classic cases showed the characteristic ChRCC copy-number pattern, only about half of the eosinophilic cases (10 of 19) showed the same, with four eosinophilic cases showing no copy-number alterations. This suggests a degree of genomic heterogeneity that distinguishes the histopathology-based classifications.

WES of 66 ChRCC cases targeted ~186,260 exons in ~18,091 genes, achieving 90% target coverage at a minimum of 20× for both tumor and matched normal samples. Overall, ChRCC displayed a low median rate of exonic somatic mutations (~0.4 per Mb) compared with most tumors (Alexandrov et al., 2013), approximately 3-fold less than the median number seen in ccRCC (which differences were also observable within

Significance

Rare diseases can provide insights into the biology of more common pathologies. Using diverse molecular platforms, we deconstructed ChRCC, a tumor characterized by slow but persistent growth and high resistance to conventional cancer therapies. Global molecular patterns provide clues as to this cancer's cell of origin. mtDNA alterations represent an integral component of the molecular portrait of ChRCC. The observed *TERT* promoter rearrangements may result from genomic instability in precancerous cells undergoing the crisis stage of immortalization, leading to activated telomerase. These data will facilitate further discovery of driver alterations extending beyond the exome as well as the generation of hypotheses that can advance our molecular understanding of this and other cancers.

Table 1. Summary of Data Types

Data Type	Platforms	Cases	Data Access
TCGA core sample set (n = 66 total cases)			
Whole-exome DNA sequence	Illumina	66	controlled
Whole-genome DNA sequence	Illumina	50	controlled
mtDNA sequence	Illumina (LR-PCR[a])	61	controlled
DNA copy number/genotype	Affymetrix SNP 6	66	controlled: CEL files
			open: copy number
mRNA expression	Illumina	66	controlled: BAM files
			open: expression
miRNA expression	Illumina	66	controlled: BAM files
			open: expression
CpG DNA methylation	Illumina 450,000 array	66	open

See also Table S1.

[a]To amplify mitochondrial DNA.

strata defined by age or stage), with the one exception showing elevated somatic mutation rate (>10/Mb by WES) and mutation signature of DNA mismatch repair deficiency (Alexandrov et al., 2013). Using alternative sequencing instrumentation, we validated 60 somatic mutation events for a set of 30 genes both arising from WES and having inferred biologically relevance (Table S2). Although our lower case numbers limited purely data-driven approaches to assigning statistical significance to infrequently mutated genes, we did have sufficient power to identify significant genes with a frequency of ~10% (Lawrence et al., 2014). Only two significant genes were thus identified (MutSig q < 0.1): *TP53* and *PTEN*.

TP53 was frequently mutated in 32% of cases (21 of the 66 profiled), with mutations correlating with decreased expression of p53 transcriptional targets (Figures S1A–S1C). *PTEN* was the next most frequently mutated, with 9% (6 of 66) nonsilent mutations detected. No other genes were found to be mutated at a frequency higher than 5%, though mutations involving cancer-relevant genes were found at lower frequencies (Figure 1B). Mutations were seen in *MTOR* (2 cases), *NRAS* (1 activating mutation), and *TSC1* or *TSC2* (4 cases), and two homozygous deletions were seen in *PTEN*, indicating that genomic targeting of the mTOR pathway occurred overall in 15 (23%) of 66 ChRCCs (Figure 1B). Biological significance could be ascribed to infrequently mutated genes, in terms of associated pathways, including the p53 and PTEN pathways (Table S2). The genetic diseases BHD and tuberous sclerosis complex both predispose to the development of ChRCC, and associated mutations converge in activation of the PTEN signaling pathway. Our study focused on sporadic disease, and a surprisingly high percentage (~47%) of our core cases did not show alterations associated with either PTEN or p53 pathways. Because no additional pathways involving sizable numbers of cases could be implicated from the exome data, our search was extended to mtDNA and structural variant (SV) analysis, as described below.

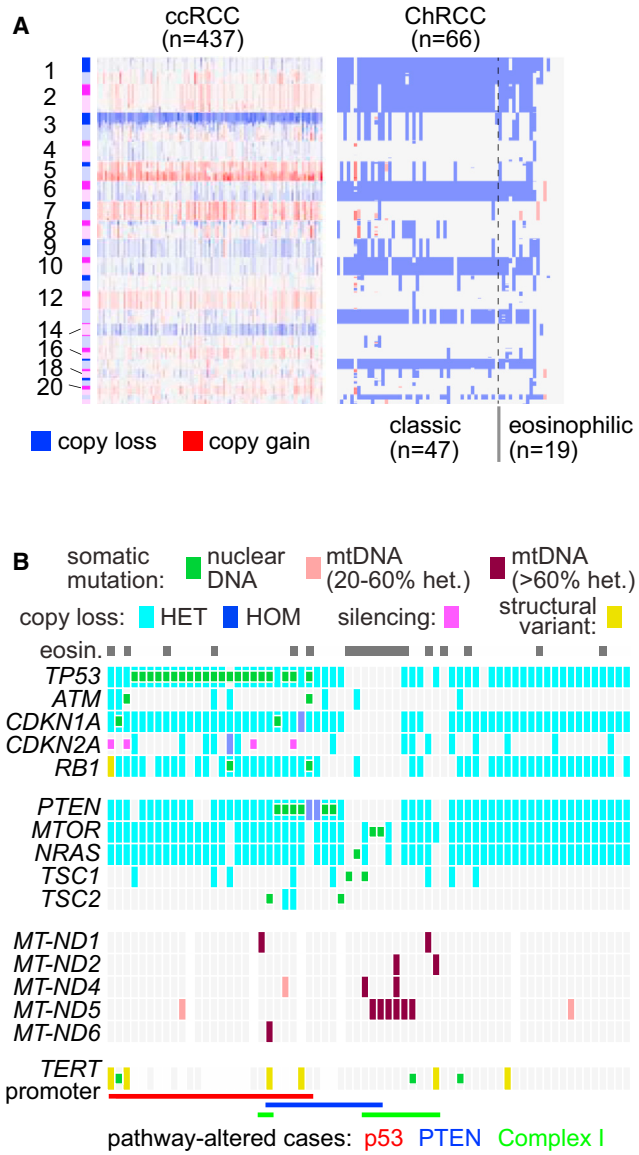

Figure 1. Gene Mutations and Copy Alterations in ChRCC

(A) Copy-number alterations (red, gain; blue, loss of one copy) by cytoband region (marker: darker color, p arm; lighter color, q arm) in ChRCC and ccRCC.

(B) Genomic alterations in ChRCC samples, each column representing a sample.

See also Figure S1 and Table S2.

DNA Methylation and RNA Analysis

TCGA data platforms allow for comparisons between tumor types (Cancer Genome Atlas Research Network et al., 2013). For example, we observed widespread differences in DNA methylation between ChRCC and ccRCC (Figure 2A), involving over 64,000 loci out of ~450,000 profiled ($p < 0.001$, t test using logit-transformed data, beta value difference > 0.1). ChRCC displayed more hypomethylation and fewer hypermethylation events compared with ccRCC. We also observed epigenetic silencing of *CDKN2A*/p16 in four ChRCC cases (Figure 2B). In principle, differential DNA methylation patterns could involve

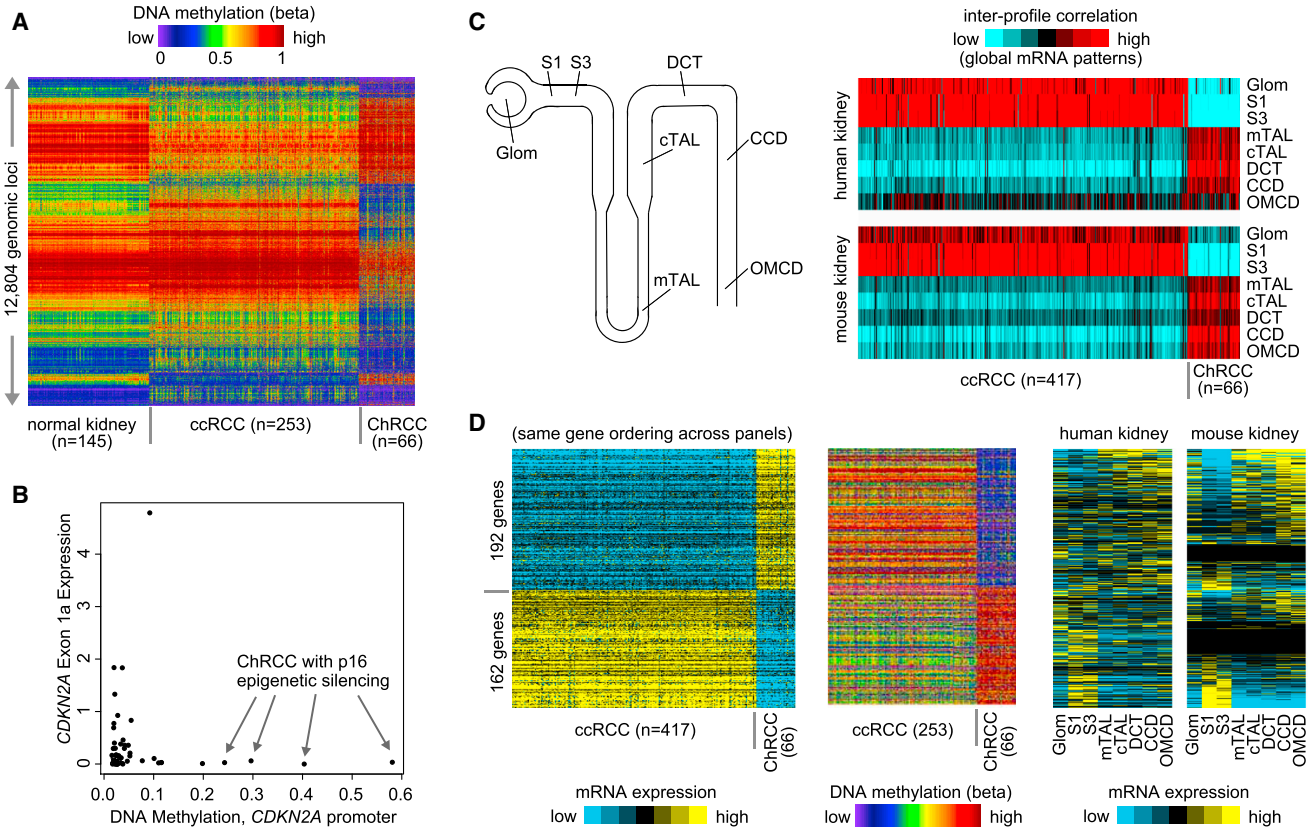

Figure 2. DNA Methylation and Gene Expression Differences between ChRCC and ccRCC

(A) Heatmap showing a randomly selected 20% of a total of 64,021 DNA methylation loci in normal kidney, ChRCC, and ccRCC (red, high; blue, low).

(B) Epigenetic silencing of *CDKN2A* locus in four ChRCC cases. Exon 1a expression corresponds to p16INK4a isoform.

(C) A cartoon of nephron (left) and heatmaps showing intersample correlations (red, positive) between profiles of kidney tumors (columns; TCGA data, arranged by subtype) and profiles of kidney nephron sites (rows; data set from Cheval et al., 2012). CCD, kidney cortical collecting duct; CNT, kidney connecting tubule; CTAL, kidney cortical thick ascending limb of Henle's loop; DCT, kidney distal convoluted tubule; Glom, kidney glomerulus; MTAL, kidney medullary thick ascending limb of Henle's loop; OMCD, kidney outer medullary collecting duct; S1/S3, kidney proximal tubule.

(D) Genes showing coordinate methylation and expression changes between ChRCC and ccRCC, with the corresponding patterns in the nephron by anatomical site.

See also Figure S2 and Tables S3, S4, and S5.

cancer-relevant pathways but may also reflect the cell of origin of the cancer (Shen and Laird, 2013). On the basis of immunohistochemical analyses (Prasad et al., 2007), ChRCC has been postulated to arise from intercalated cells in the distal convoluted tubule of the nephron, while ccRCC is thought to arise from cells in the proximal convoluted tubule; however, this issue has remained unresolved. The above DNA methylation patterns were consistent with distinct origins, leading us to further explore these origins using gene expression data.

We examined our gene expression data in the context of an external gene expression data set of normal tissue microdissected from various regions of the nephron (Cheval et al., 2012). Supervised analysis, globally comparing each TCGA ChRCC or ccRCC tumor expression profile (n = 66 and n = 417, respectively) with that of each sample in the nephron atlas, showed high mRNA expression correlations for ChRCC with distal regions of the nephron. ccRCC gene expression, however, was correlated with patterns associated with the proximal nephron (Figure 2C). These associations were also evident when focusing on the subset of differential genes in ChRCC versus ccRCC associated with inverse DNA methylation changes (Figure 2D). These results put into context many of the widespread molecular differences between these two kidney cancer types, as well as suggesting that cancers may be defined in part by cell of origin in addition to genetic aberrations.

In addition to widespread differences in gene expression between ChRCC and ccRCC, and differences from normal kidney (Figure S2A and Table S3), unsupervised clustering of mRNA profiles indicated further molecular heterogeneity within ChRCC, with at least two subsets identified (Figure S2B) as defined by differential gene expression patterns. Cluster analysis of microRNA (miRNA) profiles also indicated heterogeneity (Figure S2C), and we could identify anticorrelations between miRNAs and their predicted mRNA targets (Table S4), including an anticorrelation (false discovery rate [FDR] < 0.01) involving miR-145 (low in ChRCC versus normal) and the complex I-associated *NDUFA4* gene (Figure S2D) (Kano et al., 2010). Molecular correlates of patient survival in ChRCC were identifiable at levels of

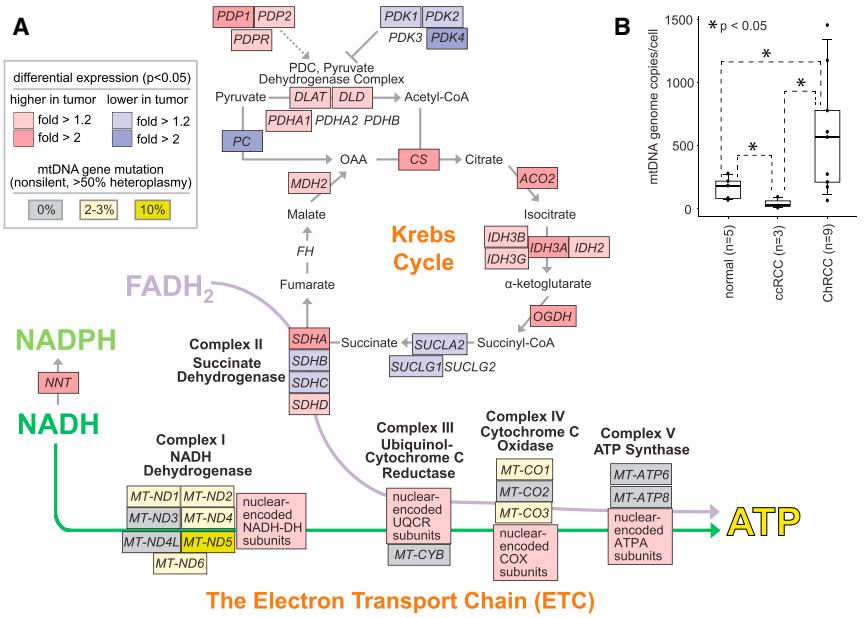

Figure 3. Molecular Alterations in ChRCC Involve Mitochondria

(A) Mutations and gene expression differences between ChRCC and normal kidney in the context of the mitochondrion. Red and blue shading represents increased and decreased expression of nuclear-encoded genes, respectively, in ChRCC; two-sided t test and fold change by unpaired analysis. Mutation rates are also indicated for mtDNA-encoded genes (not evaluated for expression): gray, no mutation; yellow, mutations detected.

(B) mtDNA copy-number analysis; p value by two-sided t test with unequal variance. Box plots represent 5%, 25%, median, 75%, and 95%.

See also Figure S3.

mRNA, miRNA, and DNA methylation (Table S5); many of these correlates were shared with those previously observed for ccRCC (Cancer Genome Atlas Research Network, 2013) and included cell cycle genes, but not the "Warburg effect"-like patterns of aggressive ccRCC (Cancer Genome Atlas Research Network, 2013).

Pathway and mtDNA Analysis

When viewed in the context of mitochondrial function, expression of nuclear-encoded genes in ChRCC, with compared to normal kidney, suggested increased utilization of the Krebs cycle and electron transport chain (ETC) for ATP generation (Figure 3A; Figures S3A and S3B). In ChRCC, nearly all genes encoding enzymes in the Krebs cycle showed increased expression over normal, with the entry of pyruvate into the Krebs cycle via acetyl coenzyme A likely through the pyruvate dehydrogenase complex. Concordantly, all complexes of the ETC demonstrated mRNA increases in at least one gene. These patterns could reflect an increased level of mitochondrial biosynthesis, resulting in greater numbers of mitochondria within each tumor cell; this possibility is supported by both the increased expression of mitochondrial biogenesis regulator *PPARGC1A* ($p < 1 \times 10^{-5}$, t test using log-transformed data; Table S3) and increased mitochondrial genome copy numbers (four times more on average in ChRCC versus normal kidney; Figure 3B; Figure S3C). These findings interestingly parallel the eosinophilic histology observed in some ChRCC, corresponding to the high uptake of eosin by mitochondria. Eosinophilic ChRCC tumors share many features with the benign variant oncocytoma, which is also characterized by dense accumulations of mitochondria (Amin et al., 2008; Tickoo et al., 2000). Furthermore, the gene expression landscape appeared very different from that of ccRCC, in which expression of genes involved in mitochondrial functions is strongly suppressed (Figure S3D) (Cancer Genome Atlas Research Network, 2013). These findings suggest that various bioenergetics strategies may support tumor growth and that not all cancers necessarily seek to minimize their reliance upon oxidative phosphorylation (Cancer Genome Atlas Research Network, 2013).

Given the indicated prevalent role of mitochondria in ChRCC and the likelihood of rapid mitochondrial genome replication (Figure 3B), we sequenced mtDNA from 61 of our 66 ChRCC cases, using a PCR-based amplification approach (Table S6). In all, we identified 142 somatic mutation events (i.e., not present in the normal) at various levels of heteroplasmy (i.e., mixture with other variants), 75 of these residing within the commonly altered D-loop noncoding region (Chatterjee et al., 2006). Thirty-five mutation events (involving 27 cases) were present in over 50% of mtDNA copies in the tumor (>50% heteroplasmy) (Figure 4A). Human mtDNA encodes 13 proteins involved in respiration and oxidative phosphorylation (Figure 3A), and we found 15 nonsilent mutations in 12 ChRCC cases involving these genes (>50% heteroplasmy), all of which validated using alternative strategies, including whole-genome sequencing (WGS)-based analysis (Larman et al., 2012) (Table S6). On the basis of previous functional studies in oncocytoma (Gasparre et al., 2008; Mayr et al., 2008; Simonnet et al., 2003), and because many of our variants represented frameshift substitutions, these mtDNA mutations are thought, in general, to lead to inactivation, rather than activation, of the associated protein.

ETC complex I genes were altered in 18% of cases (n = 11; Figures 1B and 3A; Table S3); the most frequently altered gene was *MT-ND5*, in six cases (all with >70% heteroplasmy), with five of these being histologically classified as eosinophilic ChRCC ($p < 0.01$, one-sided Fisher's exact test) and three showing no copy-number abnormalities ($p < 0.002$). *MT-ND5* is essential for the activity of complex I (Chomyn, 2001), which is responsible for the transfer of electrons from NADH to ubiquinone. One ChRCC case had a single base insertion at position 12417 that changes the length of an 8-bp homopolymer tract in *MT-ND5*, which has been observed previously in several other cancer types (Larman et al., 2012); another case had an insertion at 12384, at which position a mutation was found elsewhere in oncocytoma and associated with loss of complex I activity (Mayr et al., 2008). Two ChRCC cases each had single-base deletions at position 13230 of *MT-ND5*, but no other mtDNA

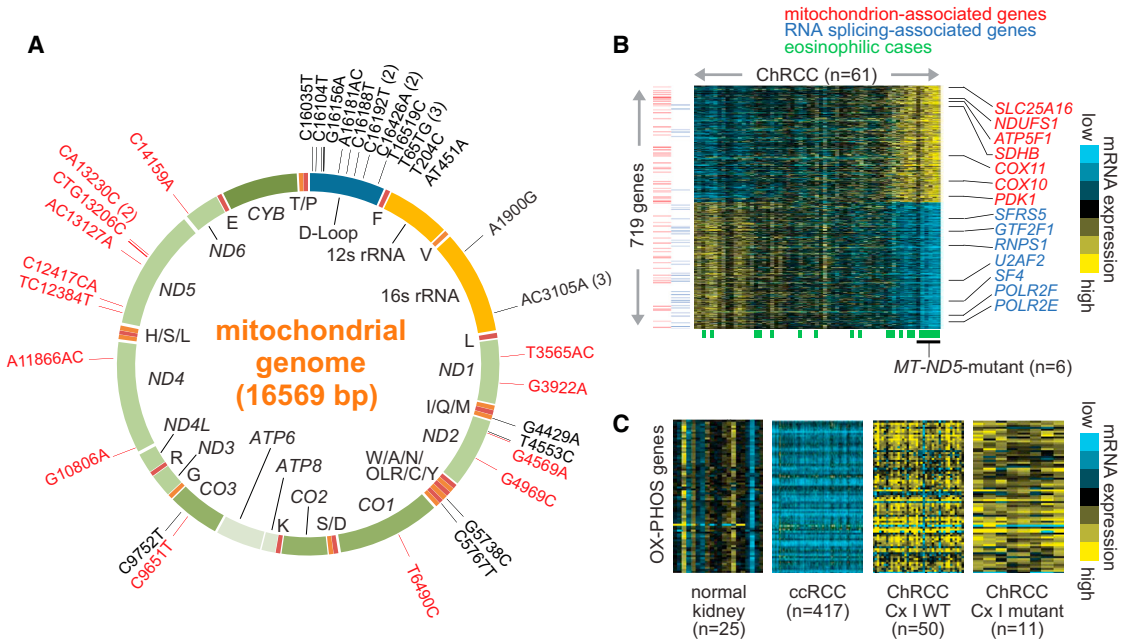

Figure 4. Integrative Analysis of mtDNA Mutations in ChRCC

(A) mtDNA somatic mutations (with >50% heteroplasmy) in 61 ChRCCs, by LR-PCR method. Red, variants that result in amino acid change.

(B) Gene expression difference (719 genes with $p < 0.001$ by t test, FDR < 0.05) between ChRCC cases harboring *MT-ND5* mutations in most mtDNA copies (>70% heteroplasmy) versus other ChRCCs.

(C) Expression of nuclear-encoded subunits of complexes I to V, or "OX-PHOS," in ChRCC and ccRCC, with (>50% heteroplasmy) or without harboring complex I (Cx I) mutations, relative to normal kidney.

See also Figure S4 and Table S6.

mutations were recurrent in our cases. We also found *MT-ND5*-mutated ChRCC cases to have a distinct gene transcription signature (Figure 4B; Figures S4A and S4B; 719 genes with $p < 0.001$ by t test, FDR < 0.05), which was shared by other eosinophilic cases and not limited to genes in regions of recurrent copy-number abnormality (Figure S4C). Genes with high expression in *MT-ND5*-mutated cases were enriched for those associated with mitochondria (43 with Gene Ontology term "mitochondrion;" $p < 5 \times 10^{-6}$, one-sided Fisher's exact test), including several with roles in ETC (*SDHB*, *NDUFS1*, *ATP5F1*, *COX10*, and *COX11*; Table S3). Notably, mutations in complex I did not result in expression patterns associated with loss of oxidative phosphorylation (Figure 4C), as might be assumed (Larman et al., 2012), suggesting possible alternative roles for complex I alteration in cancer-associated metabolic activity (Figure S4D). The associations made here, involving mtDNA mutations with mitochondrial abundance and differential gene expression patterns (which may be unique to ChRCC and related cancers), could perhaps suggest either a compensatory role for loss of complex I function or selective pressures operating to promote alternative pathways.

Whole-Genome Analysis

WGS for 50 of our 66 ChRCC cases was performed (60× and 30× coverage for paired tumor and normal, respectively). The Meerkat algorithm (Yang et al., 2013) was applied to detect genomic rearrangements, with an average of 16 found per case (range 0–207; Figure S5A), but without involving recurrent gene-gene fusions. By WGS analysis, a subset of ChRCC manifested kataegis (Figure 5A; Figure S5B), a phenomenon involving highly localized substitution mutations (C > T or C > G). Consistent with observations in other cancers (Alexandrov et al., 2013; Nik-Zainal et al., 2012), we found that regions of kataegis in ChRCC were in the vicinity of genomic rearrangements (Figure 5A; Figure S5B; average of 150 rearrangements by pter/qter region). Three ChRCC WGS profiles showed particularly strong patterns involving chromosomal region 3p, 5p, 5q, 8q, 13q, or 15q (Figure 5B). A mutation signature consistent with APOBEC cytidine deaminase activity (Alexandrov et al., 2013; Roberts et al., 2013) was significantly enriched in kataegis regions as well as in tightly spaced mutation clusters forming kataegis events (Figures S5C–S5F and Table S7). Although not detectable in ChRCC WES data (Alexandrov et al., 2013), WGS mutation spectra of six ChRCC cases, including the three with strong kataegis patterns, showed statistically significant (albeit moderate) APOBEC-patterned mutagenesis across the entire genome (Figure S5C). *APOBEC3B* mRNA expression was also elevated in ChRCC compared with normal kidney (Figure S5G).

We compared gene expression profiles between ChRCC cases with and without a strong kataegis pattern (n = 3 and n = 47, respectively) and identified 29 differentially expressed genes (FDR < 0.05) including *TERT* ($p < 1 \times 10^{-10}$, t test, FDR $< 1 \times 10^{-6}$; Figure 5C). The *TERT* gene itself showed a wide range of expression levels across ChRCC, from undetectable to hundreds of units by RNA sequencing. Focusing our

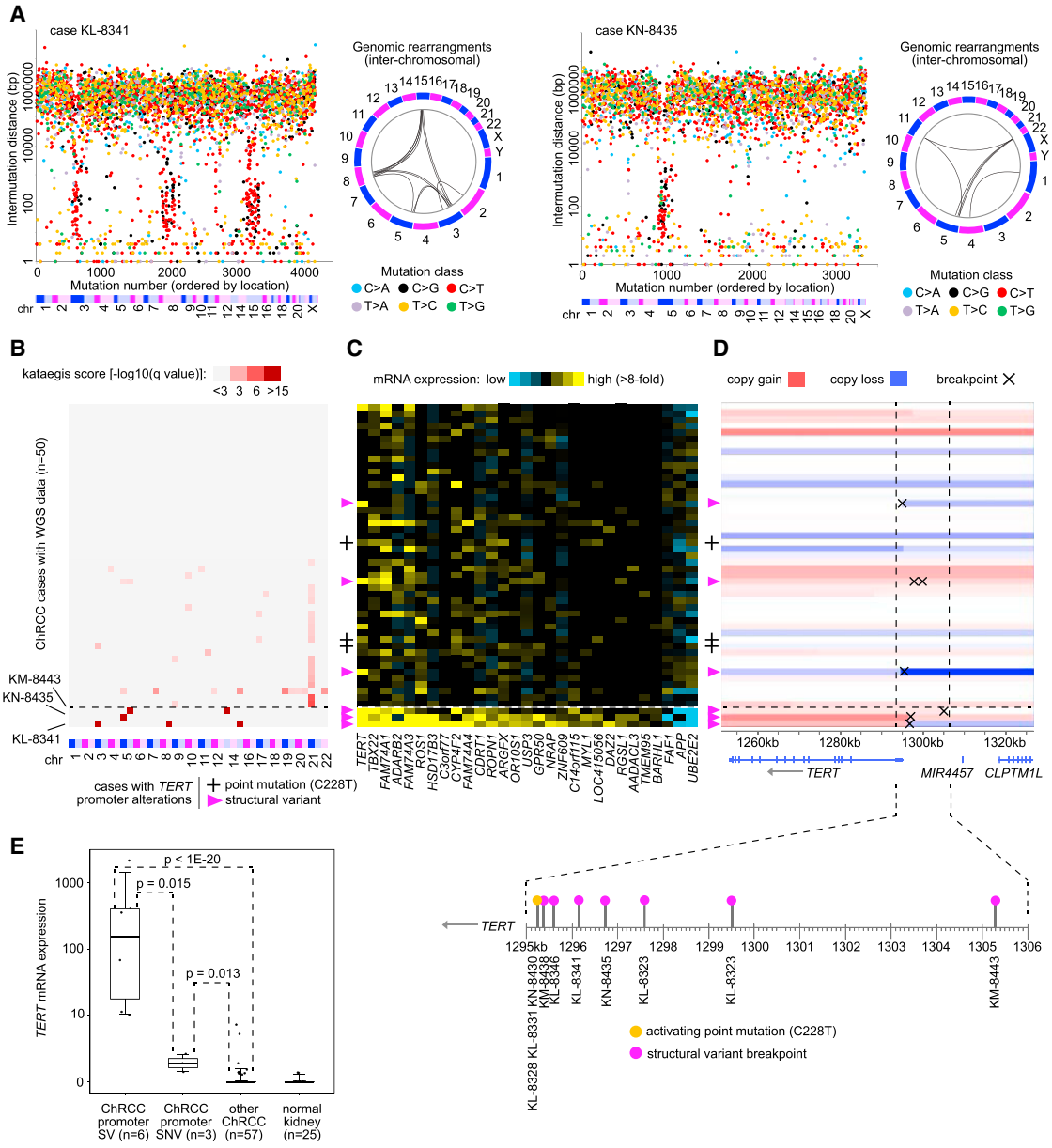

Figure 5. Kataegis and *TERT* in ChRCC

(A) Examples of a strong kataegis pattern in two ChRCC cases. "Rainfall" plots of mutations by WGS order events by genomic location. Vertical axis denotes genomic distance of each mutation from the previous mutation.

(B) WGS profiles for 50 ChRCC cases, each scored by genomic region (chromosome pter/qter) for kataegis. The 3 ChRCC cases scoring particularly strong are indicated at the bottom. Score for a given region represents a one-sided Fisher's exact test, for enrichment of C > T or C > G mutations involving intermutation distances below 10 kb (corrected for testing of multiple regions).

(C) A set of 29 differentially expressed genes (FDR < 0.05), including *TERT*, observed in ChRCC cases with strong kataegis versus other ChRCC.

(D) Copy variation and DNA breakpoint analysis identifying genomic rearrangements involving the promoter region of *TERT* for the 50 ChRCC cases (case ordering the same for B, C, and D). The 6 cases harboring rearrangements involving *TERT* are indicated (pink triangles).

(E) *TERT* expression levels in the ChRCC cases with *TERT* promoter SV, in the ChRCC cases with *TERT* promoter mutation (SNV), and in the remaining cases, as well as in normal kidney samples; p values by two-sided t test on log-transformed data. Box plots represent 5%, 25%, median, 75%, and 95%.

See also Figure S5 and Table S7.

attention on *TERT*, we sequenced the promoter region for recently identified mutations (C228T and C250T) (Huang et al., 2013); three cases harbored C228T mutations but were associated with only marginal *TERT* expression levels (average expression ~1 unit). WGS analysis of DNA copy within the *TERT* region identified some copy-number variation, but not at levels that would account for the extent of deregulated expression. However, multiple cases did show abrupt changes in copy number,

Table 2. SVs Associated with *TERT* Promoter Region by WGS Analysis

	Breakpoint A			Breakpoint B				TERT	
Case	chr:pos	ori[a]	Gene (Intron)	chr:pos	ori	Gene	Event Type	Expression[b]	Confirmed[c]
KL-8341	5:1116986	−1		5:1296148	1	TERT PM	tandem duplication	2,169.87	yes
KN-8435	5:272199	1	PDCD6 (I1)	5:1296716	1	TERT PM	inversion	417.42	yes
KM-8438	5:1348783	−1		5:1295372	1	TERT PM	deletion	356.10	yes
KL-8346	5:1125430	−1		5:1295604	1	TERT PM	tandem duplication	67.50	yes
KL-8323	5:49560803	1		5:1299528	−1	TERT PM	tandem duplication	10.37	yes
KL-8323	5:49563017	−1		5:1297603	1	TERT PM	deletion-insertion	10.37	no
KM-8443	13:52688659	1	NEK5 (I4)	5:1305300	1	TERT PM	interchromosomal translocation	9.13	yes

See also Figure S7.

[a]Denotes whether the upstream (+1) or downstream (−1) sequence was fused relative to the given coordinates.

[b]Across 66 ChRCC cases, 90th percentile of expression for TERT mRNA was 5.28 units by RNA sequencing.

[c]Confirmation using PCR across breakpoint junction, with subsequent sequencing of PCR product by PacBio platform. No PCR product was successfully obtained for one of the two breakpoints for KL-8323, likely due in part to the complexity of rearrangements in this case.

at points that fell within the region 10 kb upstream of the *TERT* transcription start site (Figure 5D). This observation suggested the existence of structural breakpoints, leading us to reexamine our Meerkat-generated results with greater scrutiny.

Subsequent WGS analysis identified genomic rearrangements involving the *TERT* promoter region, leading to breakpoints within the region in six out of 50 ChRCC cases (Figure 5D and Table 2); these cases also had the highest levels of *TERT* expression (average > 500 units, $p < 1 \times 10^{-20}$, t test; Table 2 and Figure 5E), even compared with cases with 228T mutation, and three showed the strongest manifestation of kataegis ($p = 0.001$, one-sided Fisher's exact). In five ChRCC cases, the *TERT*-associated rearrangements were intrachromosomal (one involving part of *PDCD6*), while the sixth case involved *NEK5* on chromosome 13. When considering intratumor heterogeneity, in most cases, these variants were estimated to reside in nearly all of the cells (when counting the numbers of concordant versus discordant read pairs), which would indicate that the *TERT*-associated rearrangements represent early events and therefore possible drivers. Of the seven rearrangements identified by WGS, we confirmed six (involving six cases) by PCR, by designing primers that spanned both sides of the breakpoint junction (Figure 6A; Table S8), allowing amplification of DNA spanning the breakpoint region in the tumor sample (Figure 6B; Figure S6); subsequent sequencing of the PCR product independently confirmed the junction in each case (Figure 6C). Although point mutations in the *TERT* promoter, leading to upregulation of *TERT* itself, have been recently reported in cancers such as melanoma (Heidenreich et al., 2014; Huang et al., 2013), our results represent another phenomenon, of recurrent genomic rearrangement breakpoints in the *TERT* promoter being associated with elevated *TERT* expression in cancer. A precise mechanism remains to be elucidated, though, as a result of rearrangement, a number of *cis*-regulatory elements were found to be placed in close proximity to the core promoter of *TERT* (Figure S7).

DISCUSSION

With this comprehensive molecular survey of ChRCC, we have made several important findings, in particular the observed recurrent genomic structural rearrangements involving the *TERT* promoter region and elevated *TERT* expression, and our results raise intriguing questions regarding cancer, involving the role of mtDNA alterations and the role of the cell of origin. The above key findings were made possible only by our comprehensive approach, whereby, for example, we had no prior hypotheses regarding *TERT* at the outset of our study. Additionally, mtDNA mutations in cancer, particularly those involving *MT-ND5* and complex I, have been hypothesized elsewhere to recapitulate the Warburg effect (Larman et al., 2012), though the corresponding expression and histological patterns observed in our data were consistent with a complex metabolic phenotype rather than simple loss of oxidative phosphorylation. Taken together, our key findings further illustrate the need to survey cancers outside of exome boundaries, for example, by incorporating WGS or mtDNA sequencing as part of an integrative, multiplatform analysis.

Through integration of molecular data from less common cancers, we can learn more about more frequently encountered diseases. Here, for example, our analysis of ChRCC led to additional insights regarding ccRCC. RCC represents a collection of highly distinct tumors arising from different lineages within the nephron, with distinct molecular and genetic features reflecting independent processes of tumorigenesis (Linehan, 2012). Given the complexity of function assigned to an organ such as the kidney, different cancers arising from this organ may not necessarily appear similar to each other (Alexandrov et al., 2013; Cancer Genome Atlas Network, 2012). Our multiplatform analyses clearly confirm that ChRCC is a distinct disease entity from, and shares little cell lineage or genomic characteristics with, ccRCC, further reinforcing the notion that disease-specific therapies are needed for rarer tumors such as ChRCC, rather than simply adopting conventional therapeutic strategies used for ccRCC. Given the clear genetic differences between ChRCC and ccRCC, our results would suggest cell of origin as a key factor in disease determination, observations that could inform future efforts to fractionate the pool of susceptible cells for ChRCC or ccRCC modeling or preventative interventions. In addition, these data will serve as a resource for future explorations of other tumors of kidney origin, such as papillary RCCs, while being broadly relevant as well to the study of other cancers,

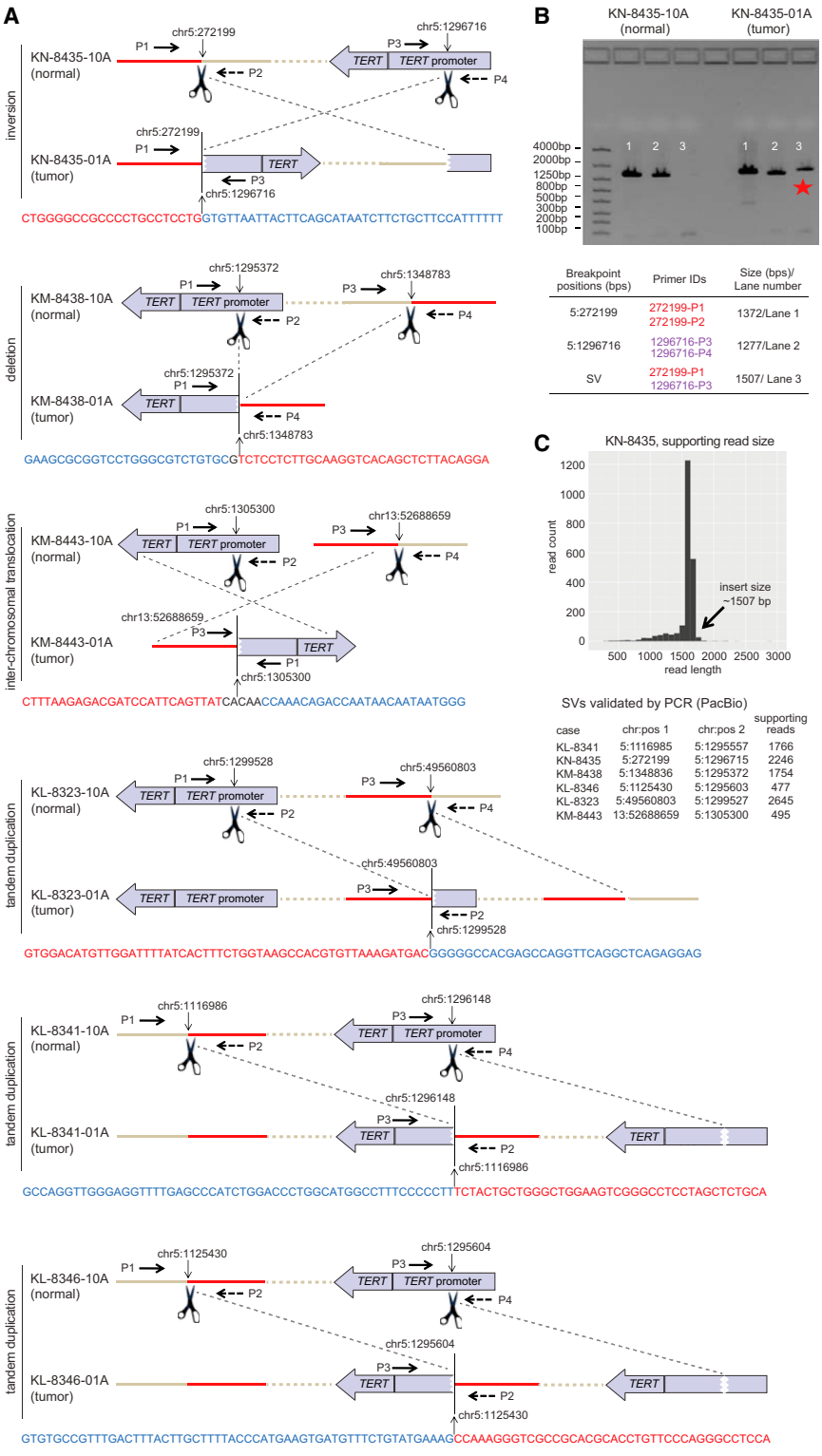

Figure 6. Genomic SVs Involving *TERT* Promoter

(A) Schematic representation of the PCR approach used to validate *TERT* promoter SVs in the six ChRCC cases and the DNA sequence surrounding the breaking point in each case. For each SV, PCR primers (P1/P2/P3/P4) were designed to span both sides of the breakpoint junction, as illustrated.

(B) For case KN-8435 (as an example), DNA spanning the SV breakpoint region could be amplified in the tumor sample (but not in the paired normal sample).

(C) For each of the six cases, amplified DNA representing SV was confirmed by sequencing (PacBio platform, which features long reads), with sufficient reads and expected length of the PCR product being observed (top, for KN-8435), and with estimated breakpoint positions being close to those of WGS results (bottom).

See also Figure S6 and Table S8.

as metabolic, genomic structural alterations, and cellular factors that influence the spectrum of genetic events contributing to cancer development are further realized.

The gene expression patterns, increased mitochondrial numbers, and histological patterns associated with ChRCC all indicate an increased importance of a distinct mitochondrial respiration program in this disease. Renal oncocytoma, a benign renal tumor that, like ChRCC, may also arise from the distal nephron, shares several similarities with ChRCC (particularly with its eosinophilic subtype), including abundant, eosinophilic cytoplasm and densely packed mitochondria (Amin et al., 2008; Tickoo et al., 2000). Mitochondrial accumulation in renal oncocytomas has been hypothesized to be a compensatory mechanism for inefficient oxidative phosphorylation (Simonnet et al., 2003), whereby loss of complex I activity may result from somatically acquired homoplasmic mutations in mitochondrial complex I genes (Gasparre et al., 2008; Mayr et al., 2008; Simonnet et al., 2003). However, gene expression in ChRCC would indicate that increased oxidative phosphorylation is maintained in complex I-altered tumors, suggesting a metabolic shift supporting the growth of this tumor, and counter to the Warburg-like phenomenon observed in high-grade, high-stage ccRCC and many other cancers (Cancer Genome Atlas Research Network, 2013), which would appear consistent with previous observations, using metabolic imaging to demonstrate uptake of radiolabeled acetate but not glucose in ChRCC (Ho et al., 2012). In general, cancer cells derive much of their ATP through oxidative phosphorylation (Ward and Thompson, 2012), and cancer-associated reprogramming of mitochondria and of other metabolic pathways, besides glycolysis and the Warburg effect, has recently received much attention (Currie et al., 2013; Ward

and Thompson, 2012). Further studies to dissect the precise role of mtDNA alterations in cancer, and mitochondrial activities promoting cancer growth, could shed light on how core metabolic pathways may be altered in ChRCC and other malignant diseases.

Our finding of recurrent DNA rearrangement breakpoints within the *TERT* promoter region in over 10% of evaluated cases represents a mechanism for increased *TERT* expression in cancer different from point mutations observed in a wide variety of cancers (Heidenreich et al., 2014; Huang et al., 2013), gene amplification (Weir et al., 2007; Chudnovsky et al., 2005), and germline polymorphisms (Rafnar et al., 2009). *TERT* is well recognized as having roles in telomere maintenance and DNA repair, in which deregulation of telomerase is a ubiquitous feature of human cancers. The previously observed *TERT* promoter mutations (C228T and C250T) create de novo E-twenty-six/ternary complex factors binding sites, which have been observed to increase transcriptional activity from the promoter by 2- to 4-fold (Huang et al., 2013). Interestingly, the *TERT* expression levels of the six cases with independently validated *TERT* promoter rearrangements were much higher than those cases with C228T promoter mutations, suggesting that these rearrangements might have an even more potent effect on upregulation of the gene. The precise mechanism of how these rearrangements affect expression remains to be elucidated; they could possibly involve rearranged *cis*-regulatory elements or could allow the core *TERT* promoter to escape from the native condensed chromatin environment (Zhao et al., 2009). The observed association of *TERT* with kataegis is also intriguing. Elsewhere, rearrangement of DNA sequences upstream of *TERT* has been reported in immortalized, nontumorigenic fibroblasts, leading to activated telomerase in cells surviving the crisis stage of immortalization (Zhao et al., 2009), which involves chromosomal instability and rearrangements due to loss of telomere capping activity; in the setting of human cancer, this would suggest that *TERT*-associated rearrangements would be involved in many cases at an early stage in tumorigenesis.

Future applications of the information presented here will include comparative analysis with other cancer types, for the possible existence elsewhere of structural rearrangements involving promoters for *TERT* or for other key drivers. As a resource with a large set of whole-genome sequences, integrated with a broad array of high-quality platform data sets, other relationships between genomic structural alterations and transcriptional components, including noncoding RNAs, remain to be uncovered. As our data represent single biopsies, future studies might focus on heterogeneity between biopsies from the same tumor (Gerlinger et al., 2012); additionally, subclonal analysis may shed light on early versus late somatic events in ChRCC tumorigenesis. Our study also revealed that divergent approaches for uncovering mtDNA mutations (long-range PCR [LR-PCR] versus WGS [Larman et al., 2012]) are highly complementary to each other, allowing WGS data from other cancers to be similarly mined for mtDNA mutations, with the additional step of combining these data with those of other platforms, in order to better understand the role of the mitochondria in cancer. Finally, the underlying data sets presented here represent part of an interlocking toolset, which can be combined with those of other cancers (Cancer Genome Atlas Research Network et al., 2013), for further discovery of driver alterations, both within and beyond the exome.

EXPERIMENTAL PROCEDURES

Patient and Sample Characteristics

With informed consent, biospecimens were collected from newly diagnosed patients with ChRCC undergoing surgical resection and who had received no prior treatment for their disease. Samples were obtained with approval from institutional review boards at Brigham and Women's Hospital, Memorial Sloan-Kettering Cancer Center, the National Cancer Institute, and The University of Texas MD Anderson Cancer Center. Using a coisolation protocol, DNA and RNA were purified. Details of sample preparation are described in Supplemental Experimental Procedures.

Data Generation

In total, 66 ChRCC cases were assayed on at least one molecular profiling platform (Table 1), which platforms included (1) RNA sequencing, (2) DNA methylation arrays, (3) miRNA sequencing, (4) Affymetrix SNP arrays, (5) WES, (6) WGS, and (7) mtDNA sequencing (using LR-PCR to amplify mtDNA). As described above and in Supplemental Experimental Procedures, both single-platform analyses and integrated cross-platform analyses were performed. Sequence files are available from CGHub (https://cghub.ucsc.edu). All other molecular, clinical, and pathological data are available through the TCGA Data Portal (https://tcga-data.nci.nih.gov/tcga/).

WGS and WES Analysis

Massively parallel sequencing exome capture was performed using NimbleGen (custom designed) VCRome 2.1 (42 MB) according the manufacturer's instructions. All exome sequencing and WGS was performed on the Illumina HiSeq platforms. Basic alignment and initial sequence analysis were carried out using the Mercury analysis pipeline (Reid et al., 2014).

mtDNA Sequencing Analysis

mtDNA was isolated from tissue samples using LR-PCR methods. Amplified mtDNA PCR products were constructed into Illumina paired-end libraries, and raw sequence data were preprocessed and aligned using the Mercury pipeline.

RNA Sequencing Analysis

Both mRNA and miRNA libraries were separately generated from total RNA and constructed using manufacturer protocols. Sequencing was done on the Illumina HiSeq platform. Read mapping and downstream data analysis were performed as described in Supplemental Experimental Procedures.

Array Data Analysis

DNA was hybridized to Affymetrix SNP 6.0 arrays and Illumina Infinium HumanMethylation450 (HM450) BeadChip arrays, according to manufacturer protocols.

SUPPLEMENTAL INFORMATION

Supplemental Information includes Supplemental Experimental Procedures, seven figures, and eight tables and can be found with this article online at http://dx.doi.org/10.1016/j.ccr.2014.07.014.

CONSORTIA

The members of the TCGA consortium are Chad J. Creighton, Caleb F. Davis, Margaret Morgan, Preethi H. Gunaratne, Lawrence A. Donehower, Benny A. Kaipparettu, David A. Wheeler, Richard A. Gibbs, Sabina Signoretti, Andrew D. Cherniack, A. Gordon Robertson, Andy Chu, Toni K. Choueiri, Elizabeth P. Henske, David J. Kwiatkowski, Victor Reuter, James J. Hsieh, A. Ari Hakimi, Satish K. Tickoo, Christopher Ricketts, W. Marston Linehan, Laura S. Schmidt, Dmitry A. Gordenin, Gyan Bhanot, Michael Seiler, Pheroze Tamboli, W. Kimryn Rathmell, Catherine C. Fahey, Kathryn E. Hacker, Angela B. Smith, Eric M. Wallen, Hui Shen, Peter W. Laird, Brian Shuch, Donna Muzny, Christian Buhay,

Min Wang, Hsu Chao, Mike Dahdouli, Liu Xi, Nipun Kakkar, Jeffrey G. Reid, Brittany Downs, Jennifer Drummond, Donna Morton, Harsha Doddapaneni, Lora Lewis, Adam English, Qingchang Meng, Christie Kovar, Qiaoyan Wang, Walker Hale, Alicia Hawes, Divya Kalra, Kimberly Walker, Bradley A. Murray, Carrie Sougnez, Gordon Saksena, Scott L. Carter, Steven E. Schumacher, Barbara Tabak, Travis I. Zack, Gad Getz, Rameen Beroukhim, Stacey B. Gabriel, Matthew Meyerson, Adrian Ally, Miruna Balasundaram, Inanc Birol, Denise Brooks, Yaron S.N. Butterfield, Eric Chuah, Amanda Clarke, Noreen Dhalla, Ranabir Guin, Robert A. Holt, Katayoon Kasaian, Darlene Lee, Haiyan I. Li, Emilia Lim, Yussanne Ma, Michael Mayo, Richard A. Moore, Andrew J. Mungall, Jacqueline E. Schein, Payal Sipahimalani, Angela Tam, Nina Thiessen, Tina Wong, Steven J.M. Jones, Marco A. Marra, J. Todd Auman, Donghui Tan, Shaowu Meng, Corbin D. Jones, Katherine A. Hoadley, Piotr A. Mieczkowski, Lisle E. Mose, Stuart R. Jefferys, Jeffrey Roach, Umadevi Veluvolu, Matthew D. Wilkerson, Scot Waring, Elizabeth Buda, Junyuan Wu, Tom Bodenheimer, Alan P. Hoyle, Janae V. Simons, Mathew G. Soloway, Saianand Balu, Joel S. Parker, D. Neil Hayes, Charles M. Perou, Daniel J. Weisenberger, Moiz S. Bootwalla, Timothy Triche Jr., Phillip H. Lai, David J. Van Den Berg, Stephen B. Baylin, Fengju Chen, Cristian Coarfa, Michael S. Noble, Daniel DiCara, Hailei Zhang, Juok Cho, David I. Heiman, Nils Gehlenborg, Doug Voet, Pei Lin, Scott Frazer, Petar Stojanov, Yingchun Liu, Lihua Zou, Jaegil Kim, Michael S. Lawrence, Lynda Chin, Lixing Yang, Sahil Seth, Christopher A. Bristow, Alexei Protopopov, Xingzhi Song, Jianhua Zhang, Angeliki Pantazi, Angela Hadjipanayis, Eunjung Lee, Lovelace J. Luquette, Semin Lee, Michael Parfenov, Netty Santoso, Jonathan Seidman, Andrew W. Xu, Raju Kucherlapati, Peter J. Park, Hyojin Kang, Junehawk Lee, Steven A. Roberts, Leszek J. Klimczak, David Fargo, Martin Lang, Yoon-La Choi, Sang Cheol Kim, June-Koo Lee, Woong-Yang Park, Wenyi Wang, Yu Fan, Jaeil Ahn, Rehan Akbani, John N. Weinstein, David Haussler, Josh M. Stuart, Christopher C. Benz, Singer Ma, Amie Radenbaugh, Jingchun Zhul, Michael Biehl, Tara M. Lichtenberg, Erik Zmuda, Aaron D. Black, Benjamin Hanf, Nilsa C. Ramirez, Lisa Wise, Jay Bowen, Kristen M. Leraas, Tracy M. Hall, Julie M. Gastier-Foster, William G. Kaelin, Leigh Thorne, Lori Boice, Mei Huang, Cathy Vocke, James Peterson, Robert Worrell, Maria Merino, Bogdan A. Czerniak, Kenneth D. Aldape, Christopher G. Wood, Paul T. Spellman, Michael B. Atkins, John Cheville, R. Houston Thompson, Mark A. Jensen, Todd Pihl, Yunhu Wan, Brenda Ayala, Julien Baboud, Sudhakar Velaga, Jessica Walton, Jia Liu, Sudha Chudamani, Ye Wu, Margi Sheth, Kenna R. Mills Shaw, John A. Demchok, Tanja Davidsen, Liming Yang, Zhining Wang, Roy W. Tarnuzzer, Jiashan Zhang, Greg Eley, Ina Felau, Jean Claude Zenklusen, Carolyn M. Hutter, Mark S. Guyer, Bradley A. Ozenberger, and Heidi J. Sofia.

AUTHOR CONTRIBUTIONS

The TCGA consortium contributed collectively to this study. Biospecimens were provided by the Tissue Source Sites and processed by the Biospecimen Core Resource. Data generation and analyses were performed by the Genome Sequencing Center, Genome Characterization Centers, and Genome Data Analysis centers. All data were released through the Data Coordinating Center. Project activities were coordinated by the National Cancer Institute and National Human Genome Research Institute Project Teams. Initial guidance in the project design was provided by the Disease Working Group. We also acknowledge the following TCGA investigators of the Analysis Working Group, who contributed substantially to the analysis and writing of this manuscript: project leaders: C.J.C. and W.K.R.; data coordinator: M.M.; manuscript coordinator: B.S.; analysis coordinator: C.J.C.; writing team: C.J.C., R.A.G., E.P.H., D.J.K., W.M.L., W.K.R., C.J.R., and B.S.; DNA sequence analysis: C.F.D., D.A.G., H.K., S.C.K., P.J.P., D.A.W., and L.Y.; mRNA analysis: G.B., M.B., C.C.F., and K.E.H.; miRNA analysis: A.C., P.H.G., and A.G.R.; DNA methylation analysis: H.S. and P.W.L.; copy-number analysis: A.D.C.; mitochondrial analysis: D.M., C.A.B., C.B., B.A.K., S.S., and M.W.; pathway analysis: L.A.D., D.J.K., and C.J.R.; clinical data: A.B.S. and E.M.W.; pathology and clinical expertise: T.K.C., A.A.H., E.P.H., J.J.H., W.M.L., W.K.R., V.R., L.S.S., B.S., P.T., and S.K.T.

ACKNOWLEDGMENTS

We wish to thank all patients and families who contributed to this study. This work was supported by the following grants from the NIH: 5U24CA143843 (D.A.W.), U54HG003273 (R.A.G.), 5U24CA143866 (M.A. Marra), KL2TR001109 and UL1TR001111 (A.B.S.), 5P50CA101942 (S. Signoretti), 5P50CA101942 (T.K.C.), U54 HG003067 (E. Lander); K24CA172355 (W.K.R.), Intramural Research Program of the NIH, National Cancer Institute, Center for Cancer Research (W.M.L., L.S.S., C.J.R., M.J. Merino), with federal funds from the Frederick National Lab, NIH, under contract HHSN261200800001E (L.S.S.), Intramural Research Program of the NIH, National Institute of Environmental Health Sciences (D.A.G., S.A. Roberts, L.J. Klimczak, D. Fargo), and a training fellowship from the Keck Center for Interdisciplinary Bioscience Training of the Gulf Coast Consortia (Grant No. T15 LM007093 to C.F.D.). Other grant support includes the J. Randall & Kathleen L. MacDonald Kidney Cancer Research Fund, the Tuttle Family Kidney Cancer Research Fund (J.J.H.), the Korean Health Technology R&D Project, Ministry of Health & Welfare, Republic of Korea (HI13C2096 to W.-Y.P.), and the Korea Institute of Science and Technology Information (K-14-L01-C02-S04 and KSC-2013-C3-037) (for supercomputing resources including technical support).

Received: April 24, 2014
Revised: June 29, 2014
Accepted: July 17, 2014
Published: August 21, 2014

REFERENCES

Alexandrov, L.B., Nik-Zainal, S., Wedge, D.C., Aparicio, S.A., Behjati, S., Biankin, A.V., Bignell, G.R., Bolli, N., Borg, A., Børresen-Dale, A.L., et al.; Australian Pancreatic Cancer Genome Initiative; ICGC Breast Cancer Consortium; ICGC MMML-Seq Consortium; ICGC PedBrain (2013). Signatures of mutational processes in human cancer. Nature *500*, 415–421.

Amin, M.B., Amin, M.B., Tamboli, P., Javidan, J., Stricker, H., de-Peralta Venturina, M., Deshpande, A., and Menon, M. (2002). Prognostic impact of histologic subtyping of adult renal epithelial neoplasms: an experience of 405 cases. Am. J. Surg. Pathol. *26*, 281–291.

Amin, M.B., Paner, G.P., Alvarado-Cabrero, I., Young, A.N., Stricker, H.J., Lyles, R.H., and Moch, H. (2008). Chromophobe renal cell carcinoma: histomorphologic characteristics and evaluation of conventional pathologic prognostic parameters in 145 cases. Am. J. Surg. Pathol. *32*, 1822–1834.

Brunelli, M., Eble, J.N., Zhang, S., Martignoni, G., Delahunt, B., and Cheng, L. (2005). Eosinophilic and classic chromophobe renal cell carcinomas have similar frequent losses of multiple chromosomes from among chromosomes 1, 2, 6, 10, and 17, and this pattern of genetic abnormality is not present in renal oncocytoma. Mod. Pathol. *18*, 161–169.

Cancer Genome Atlas Network (2012). Comprehensive molecular portraits of human breast tumours. Nature *490*, 61–70.

Cancer Genome Atlas Research Network (2013). Comprehensive molecular characterization of clear cell renal cell carcinoma. Nature *499*, 43–49.

Cancer Genome Atlas Research Network, Weinstein, J., Collisson, E., Mills, G., Shaw, K., Ozenberger, B., Ellrott, K., Shmulevich, I., Sander, C., and Stuart, J. (2013). The Cancer Genome Atlas Pan-Cancer analysis project. Nat. Genet. *45*, 1113–1120.

Chatterjee, A., Mambo, E., and Sidransky, D. (2006). Mitochondrial DNA mutations in human cancer. Oncogene *25*, 4663–4674.

Cheval, L., Pierrat, F., Rajerison, R., Piquemal, D., and Doucet, A. (2012). Of mice and men: divergence of gene expression patterns in kidney. PLoS ONE *7*, e46876.

Chomyn, A. (2001). Mitochondrial genetic control of assembly and function of complex I in mammalian cells. J. Bioenerg. Biomembr. *33*, 251–257.

Chudnovsky, Y., Adams, A., Robbins, P., Lin, Q., and Khavari, P. (2005). Use of human tissue to assess the oncogenic activity of melanoma-associated mutations. Nat. Genet. *37*, 745–749.

Currie, E., Schulze, A., Zechner, R., Walther, T.C., and Farese, R.V.J., Jr. (2013). Cellular fatty acid metabolism and cancer. Cell Metab. *18*, 153–161.

Gasparre, G., Hervouet, E., de Laplanche, E., Demont, J., Pennisi, L.F., Colombel, M., Mège-Lechevallier, F., Scoazec, J.Y., Bonora, E., Smeets, R., et al. (2008). Clonal expansion of mutated mitochondrial DNA is associated

with tumor formation and complex I deficiency in the benign renal oncocytoma. Hum. Mol. Genet. *17*, 986–995.

Gerlinger, M., Rowan, A.J., Horswell, S., Larkin, J., Endesfelder, D., Gronroos, E., Martinez, P., Matthews, N., Stewart, A., Tarpey, P., et al. (2012). Intratumor heterogeneity and branched evolution revealed by multiregion sequencing. N. Engl. J. Med. *366*, 883–892.

Heidenreich, B., Rachakonda, P.S., Hemminki, K., and Kumar, R. (2014). TERT promoter mutations in cancer development. Curr. Opin. Genet. Dev. *24*, 30–37.

Ho, C.L., Chen, S., Ho, K.M., Chan, W.K., Leung, Y.L., Cheng, K.C., Wong, K.N., Cheung, M.K., and Wong, K.K. (2012). Dual-tracer PET/CT in renal angiomyolipoma and subtypes of renal cell carcinoma. Clin. Nucl. Med. *37*, 1075–1082.

Huang, F.W., Hodis, E., Xu, M.J., Kryukov, G.V., Chin, L., and Garraway, L.A. (2013). Highly recurrent TERT promoter mutations in human melanoma. Science *339*, 957–959.

Jemal, A., Simard, E.P., Dorell, C., Noone, A.M., Markowitz, L.E., Kohler, B., Eheman, C., Saraiya, M., Bandi, P., Saslow, D., et al. (2013). Annual Report to the Nation on the Status of Cancer, 1975-2009, featuring the burden and trends in human papillomavirus(HPV)-associated cancers and HPV vaccination coverage levels. J. Natl. Cancer Inst. *105*, 175–201.

Kano, M., Seki, N., Kikkawa, N., Fujimura, L., Hoshino, I., Akutsu, Y., Chiyomaru, T., Enokida, H., Nakagawa, M., and Matsubara, H. (2010). miR-145, miR-133a and miR-133b: Tumor-suppressive miRNAs target FSCN1 in esophageal squamous cell carcinoma. Int. J. Cancer *127*, 2804–2814.

Larman, T.C., DePalma, S.R., Hadjipanayis, A.G., Protopopov, A., Zhang, J., Gabriel, S.B., Chin, L., Seidman, C.E., Kucherlapati, R., and Seidman, J.G.; Cancer Genome Atlas Research Network (2012). Spectrum of somatic mitochondrial mutations in five cancers. Proc. Natl. Acad. Sci. USA *109*, 14087–14091.

Lawrence, M.S., Stojanov, P., Mermel, C.H., Robinson, J.T., Garraway, L.A., Golub, T.R., Meyerson, M., Gabriel, S.B., Lander, E.S., and Getz, G. (2014). Discovery and saturation analysis of cancer genes across 21 tumour types. Nature *505*, 495–501.

Linehan, W.M. (2012). Genetic basis of kidney cancer: role of genomics for the development of disease-based therapeutics. Genome Res. *22*, 2089–2100.

Mayr, J.A., Meierhofer, D., Zimmermann, F., Feichtinger, R., Kögler, C., Ratschek, M., Schmeller, N., Sperl, W., and Kofler, B. (2008). Loss of complex I due to mitochondrial DNA mutations in renal oncocytoma. Clin. Cancer Res. *14*, 2270–2275.

Mermel, C.H., Schumacher, S.E., Hill, B., Meyerson, M.L., Beroukhim, R., and Getz, G. (2011). GISTIC2.0 facilitates sensitive and confident localization of the targets of focal somatic copy-number alteration in human cancers. Genome Biol. *12*, R41.

Nickerson, M.L., Warren, M.B., Toro, J.R., Matrosova, V., Glenn, G., Turner, M.L., Duray, P., Merino, M., Choyke, P., Pavlovich, C.P., et al. (2002). Mutations in a novel gene lead to kidney tumors, lung wall defects, and benign tumors of the hair follicle in patients with the Birt-Hogg-Dubé syndrome. Cancer Cell *2*, 157–164.

Nik-Zainal, S., Alexandrov, L.B., Wedge, D.C., Van Loo, P., Greenman, C.D., Raine, K., Jones, D., Hinton, J., Marshall, J., Stebbings, L.A., et al.; Breast Cancer Working Group of the International Cancer Genome Consortium (2012). Mutational processes molding the genomes of 21 breast cancers. Cell *149*, 979–993.

Pavlovich, C.P., Walther, M.M., Eyler, R.A., Hewitt, S.M., Zbar, B., Linehan, W.M., and Merino, M.J. (2002). Renal tumors in the Birt-Hogg-Dubé syndrome. Am. J. Surg. Pathol. *26*, 1542–1552.

Perou, C.M., Sørlie, T., Eisen, M.B., van de Rijn, M., Jeffrey, S.S., Rees, C.A., Pollack, J.R., Ross, D.T., Johnsen, H., Akslen, L.A., et al. (2000). Molecular portraits of human breast tumours. Nature *406*, 747–752.

Prasad, S.R., Narra, V.R., Shah, R., Humphrey, P.A., Jagirdar, J., Catena, J.R., Dalrymple, N.C., and Siegel, C.L. (2007). Segmental disorders of the nephron: histopathological and imaging perspective. Br. J. Radiol. *80*, 593–602.

Przybycin, C.G., Cronin, A.M., Darvishian, F., Gopalan, A., Al-Ahmadie, H.A., Fine, S.W., Chen, Y.B., Bernstein, M., Russo, P., Reuter, V.E., and Tickoo, S.K. (2011). Chromophobe renal cell carcinoma: a clinicopathologic study of 203 tumors in 200 patients with primary resection at a single institution. Am. J. Surg. Pathol. *35*, 962–970.

Rafnar, T., Sulem, P., Stacey, S.N., Geller, F., Gudmundsson, J., Sigurdsson, A., Jakobsdottir, M., Helgadottir, H., Thorlacius, S., Aben, K.K., et al. (2009). Sequence variants at the TERT-CLPTM1L locus associate with many cancer types. Nat. Genet. *41*, 221–227.

Reid, J.G., Carroll, A., Veeraraghavan, N., Dahdouli, M., Sundquist, A., English, A., Bainbridge, M., White, S., Salerno, W., Buhay, C., et al. (2014). Launching genomics into the cloud: deployment of Mercury, a next generation sequence analysis pipeline. BMC Bioinformatics *15*, 30.

Roberts, S.A., Lawrence, M.S., Klimczak, L.J., Grimm, S.A., Fargo, D., Stojanov, P., Kiezun, A., Kryukov, G.V., Carter, S.L., Saksena, G., et al. (2013). An APOBEC cytidine deaminase mutagenesis pattern is widespread in human cancers. Nat. Genet. *45*, 970–976.

Schmidt, L.S., Warren, M.B., Nickerson, M.L., Weirich, G., Matrosova, V., Toro, J.R., Turner, M.L., Duray, P., Merino, M., Hewitt, S., et al. (2001). Birt-Hogg-Dubé syndrome, a genodermatosis associated with spontaneous pneumothorax and kidney neoplasia, maps to chromosome 17p11.2. Am. J. Hum. Genet. *69*, 876–882.

Shen, H., and Laird, P.W. (2013). Interplay between the cancer genome and epigenome. Cell *153*, 38–55.

Shuch, B., Ricketts, C.J., Vocke, C.D., Komiya, T., Middelton, L.A., Kauffman, E.C., Merino, M.J., Metwalli, A.R., Dennis, P., and Linehan, W.M. (2013). Germline PTEN mutation cowden syndrome: an underappreciated form of hereditary kidney cancer. J. Urol. *190*, 1990–1998.

Simonnet, H., Demont, J., Pfeiffer, K., Guenaneche, L., Bouvier, R., Brandt, U., Schagger, H., and Godinot, C. (2003). Mitochondrial complex I is deficient in renal oncocytomas. Carcinogenesis *24*, 1461–1466.

Speicher, M.R., Schoell, B., du Manoir, S., Schröck, E., Ried, T., Cremer, T., Störkel, S., Kovacs, A., and Kovacs, G. (1994). Specific loss of chromosomes 1, 2, 6, 10, 13, 17, and 21 in chromophobe renal cell carcinomas revealed by comparative genomic hybridization. Am. J. Pathol. *145*, 356–364.

Störkel, S., Eble, J.N., Adlakha, K., Amin, M., Blute, M.L., Bostwick, D.G., Darson, M., Delahunt, B., and Iczkowski, K.; Union Internationale Contre le Cancer (UICC) and the American Joint Committee on Cancer (AJCC) (1997). Classification of renal cell carcinoma: Workgroup No. 1. Cancer *80*, 987–989.

Tickoo, S.K., Lee, M.W., Eble, J.N., Amin, M., Christopherson, T., Zarbo, R.J., and Amin, M.B. (2000). Ultrastructural observations on mitochondria and microvesicles in renal oncocytoma, chromophobe renal cell carcinoma, and eosinophilic variant of conventional (clear cell) renal cell carcinoma. Am. J. Surg. Pathol. *24*, 1247–1256.

Varela, I., Tarpey, P., Raine, K., Huang, D., Ong, C.K., Stephens, P., Davies, H., Jones, D., Lin, M.L., Teague, J., et al. (2011). Exome sequencing identifies frequent mutation of the SWI/SNF complex gene PBRM1 in renal carcinoma. Nature *469*, 539–542.

Ward, P.S., and Thompson, C.B. (2012). Metabolic reprogramming: a cancer hallmark even warburg did not anticipate. Cancer Cell *21*, 297–308.

Weir, B.A., Woo, M.S., Getz, G., Perner, S., Ding, L., Beroukhim, R., Lin, W.M., Province, M.A., Kraja, A., Johnson, L.A., et al. (2007). Characterizing the cancer genome in lung adenocarcinoma. Nature *450*, 893–898.

Yang, L., Luquette, L.J., Gehlenborg, N., Xi, R., Haseley, P.S., Hsieh, C.H., Zhang, C., Ren, X., Protopopov, A., Chin, L., et al. (2013). Diverse mechanisms of somatic structural variations in human cancer genomes. Cell *153*, 919–929.

Zhao, Y., Wang, S., Popova, E.Y., Grigoryev, S.A., and Zhu, J. (2009). Rearrangement of upstream sequences of the hTERT gene during cellular immortalization. Genes Chromosomes Cancer *48*, 963–974.